# Differential Metabolism of Gefitinib and Erlotinib by Human Cytochrome P450 Enzymes

Jing Li, Ming Zhao, Ping He, Manuel Hidalgo, and Sharyn D. Baker

**Abstract**

**Purpose:** To examine the enzyme kinetics of gefitinib and erlotinib metabolism by individual cytochrome P450 (CYP) enzymes, and to compare their effects on CYP3A activity, with the aim to better understand mechanisms underlying pharmacokinetic variability and clinical effects.

**Experimental Design:** Enzyme kinetics were examined by incubating gefitinib or erlotinib (1.5-50 μmol/L) with recombinant human CYP3A4, CYP3A5, CYP2D6, CYP1A1, CYP1A2, and CYP1B1 (10-160 pmol/mL). Their effects on CYP3A activity were examined by comparing midazolam metabolism in the presence and absence of gefitinib or erlotinib in human liver and intestinal microsomes. Parent compounds and metabolites were monitored by high-performance liquid chromatography with a photodiode detector or tandem mass spectrometer.

**Results:** Both drugs were metabolized primarily by CYP3A4, CYP3A5, and CYP1A1, with respective maximum clearance ($Cl_{max}$) values for metabolism of 0.41, 0.39, and 0.57 mL/min/nmol for gefitinib and 0.24, 0.21, 0.31 mL/min/nmol for erlotinib. CYP2D6 was involved in gefitinib metabolism ($Cl_{max}$, 0.63 mL/min/nmol) to a large extent, whereas CYP1A2 was considerably involved in erlotinib metabolism ($Cl_{max}$, 0.15 mL/min/nmol). Both drugs stimulated CYP3A-mediated midazolam disappearance and 1-hydroxymidazolam formation in liver and intestinal microsomes.

**Conclusions:** Gefitinib is more susceptible to CYP3A-mediated metabolism than erlotinib, which may contribute to the higher apparent oral clearance observed for gefitinib. Metabolism by hepatic and extrahepatic CYP1A may represent a determinant of pharmacokinetic variability and response for both drugs. The differential metabolizing enzyme profiles suggest that there may be differences in drug-drug interaction potential and that stimulation of CYP3A4 may likely play a role in drug interactions for erlotinib and gefitinib.

Gefitinib and erlotinib are orally bioavailable synthetic anilinoquinazolines that selectively and reversibly bind to the intracellular ATP-binding site of the epidermal growth factor receptor (EGFR) tyrosine kinase, and have shown activity in patients with non–small-cell lung cancer (1). Gefitinib and erlotinib share a common chemical backbone structure and exhibit similar disposition characteristics in humans after oral administration (1). They are reported to have similar oral bioavailability (~60%; refs. 2, 3) and undergo extensive metabolism primarily by cytochrome P450 (CYP) 3A4 (4, 5), with >80% of the administered dose excreted in feces (4, 6). Both drugs are associated with wide interindividual pharmacokinetic variability in cancer patients (7, 8). Administration of erlotinib at the maximum tolerated dose (MTD) and approved dose of 150 mg once daily achieved an approximate 3.5-fold higher steady-state plasma trough concentration than gefitinib administered at the recommended dose but approximately one third the MTD, of 250 mg once daily (1.5 versus 0.41 μg/mL; refs. 7, 9). As food intake has been shown to increase erlotinib bioavailability to ~100% (1), it is unknown if the higher erlotinib exposure observed in the study by Tan et al. (9) was due, in part, to administration of drug with food. Even so, enhancement of bioavailability from 60% to 100% by food consumption could not explain the 3.5-fold difference in plasma concentrations. Thus, gefitinib likely has lower bioavailability and/or higher systemic clearance than erlotinib. Indeed, recent population pharmacokinetic analyses showed that gefitinib has a higher apparent oral clearance than erlotinib (21 versus 4.0 L/h; refs. 7, 8).

Numerous factors, including CYP-mediated metabolism, could influence the systemic exposure achieved after oral administration of gefitinib and erlotinib. Although one study has evaluated the qualitative *in vitro* metabolism of gefitinib using human liver microsomes and recombinant CYP enzymes (5), a quantitative assessment of the affinity and capacity of individual CYP enzymes to metabolize gefitinib and erlotinib has not been done. The purpose of this study was to examine the kinetics of metabolism of gefitinib and erlotinib by

**Authors' Affiliation:** The Sidney Kimmel Comprehensive Cancer Center at Johns Hopkins, Baltimore, Maryland

Received 1/15/07; revised 3/7/07; accepted 3/22/07.

**Grant support:** NIH grant P50 AT00437 and the Commonwealth Foundation for Cancer Research.

The costs of publication of this article were defrayed in part by the payment of page charges. This article must therefore be hereby marked *advertisement* in accordance with 18 U.S.C. Section 1734 solely to indicate this fact.

**Requests for reprints:** Sharyn D. Baker, Pharmaceutical Sciences Department, St. Jude Children's Research Hospital, 332 North Lauderdale Street, DTRC Room D1034, Mail Stop 314, Memphis, TN 38105. Phone: 901-495-3089; Fax: 901-495-3125; E-mail: sharyn.baker@stjude.org.



doi:10.1158/1078-0432.CCR-07-0088

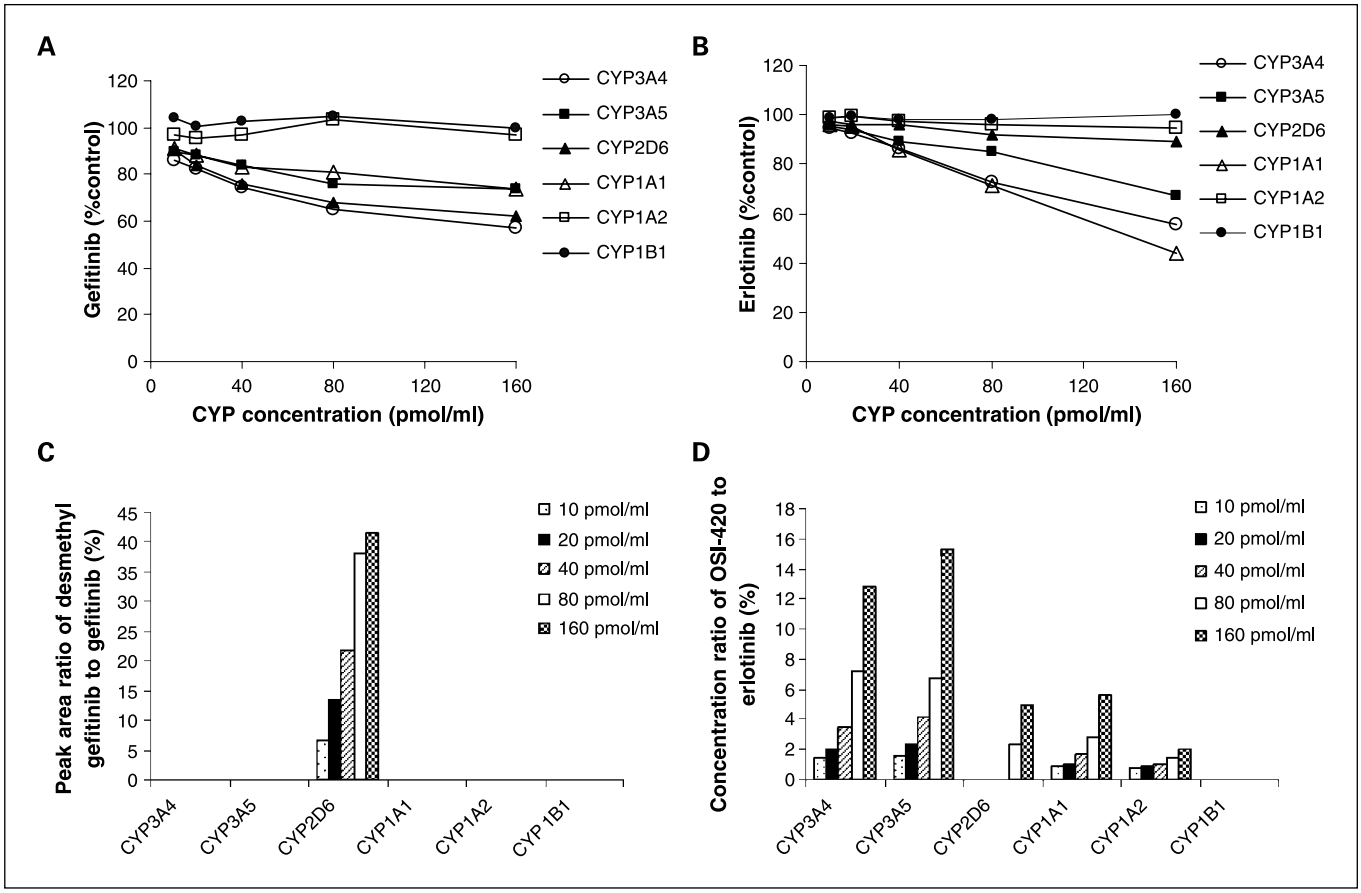


**Fig. 1.** The disappearance of gefitinib (*A*) and erlotinib (*B*) as well as formation of desmethyl gefitinib (*C*) and OSI 420 (*D*) when gefitinib or erlotinib (50 μmol/L) was incubated with human CYP3A4, CYP3A5, CYP2D6, CYP1A1, CYP1A2, and CYP1B1 Supersomes at CYP concentrations of 10 to 160 pmol/mL, at 37°C for 30 min. The control was the incubation of gefitinib or erlotinib with insect cell control Supersomes. Points, average of duplicate determinations (with coefficient variation <10%).

individual CYP enzymes, with the aim to quantitatively compare the contributions of individual CYP to their metabolism. In addition, their effects on CYP3A activity were compared by examining the metabolism of the CYP3A probe drug midazolam in the presence or absence of gefitinib or erlotinib in human liver and intestinal microsomes.

## Materials and Methods

***Chemicals.*** Gefitinib and erlotinib (OSI-774) were purchased from Toronto Research Chemicals, Inc.; erlotinib metabolite (OSI-420) was obtained from OSI Pharmaceuticals; midazolam was obtained from Sigma-Aldrich; and 1-hydroxymidazolam was bought from BD Biosciences. Human CYP3A4, CYP3A5, CYP2D6, CYP1A1, CYP1A2, and CYP1B1 Supersomes; insect cell control Supersomes; pooled human liver and intestinal microsomes; and NADPH-regenerating system solutions A and B were purchased from BD Biosciences.

**In vitro *metabolism of gefitinib and erlotinib.*** Gefitinib or erlotinib were incubated with CYP3A4, CYP3A5, CYP2D6, CYP1A1, CYP1A2, and CYP1B1 Supersomes. Reaction mixtures (total volume 0.2 mL) containing erlotinib or gefitinib, 1.3 mmol/L $NADP^+$, 3.3 mmol/L glucose-6-phosphate, 0.4 units/mL glucose-6-phosphate dehydrogenase, 3.3 mmol/L magnesium chloride, and CYP enzyme in 100 mmol/L potassium phosphate buffer (pH 7.4) were incubated at 37°C for 30 min and terminated by adding 100 μL acetonitrile and centrifugation at 14,000 rpm at 4°C for 10 min. The supernatant was collected and stored at -80°C until analysis. An incubation with control Supersomes was done simultaneously. To determine which CYP enzymes were involved in drug metabolism, 50 μmol/L erlotinib or gefitinib were incubated with increasing concentrations of CYP enzyme (10-160 pmol/mL). To evaluate the kinetics of metabolism, erlotinib (1.56-50 μmol/L) was incubated with 100 pmol/mL CYP enzyme or gefitinib (1.56-100 μmol/L) was incubated with 50 pmol/mL CYP enzyme.

Gefitinib, *O*-desmethyl-gefitinib, erlotinib, and OSI-420 (*O*-desmethyl-erlotinib) were separated and measured by high-performance liquid chromatography using a Waters Model 2690 separations system equipped with a photodiode array detector. The peak associated with *O*-desmethyl gefitinib was confirmed by fraction collection of the peak of interest and verification of the mass spectrum and product ions using a Micromass Quattro LC triple-quadrupole mass spectrometric detector (data not shown). One hundred microliters of the supernatant of the incubation mixture were injected and separated on a 4.6 × 250 mm Luna 5 μ C18 column (Phenomenex; for gefitinib) or 3.9 × 150 mm SymmetryShield $RP_8$ column (Waters; for erlotinib) with a mobile phase consisting of acetonitrile-0.4% ammonium acetate (40:60, v/v; for gefitinib) or acetonitrile-0.05 mol/L potassium phosphate buffer (pH 4.8, 32:68, v/v; for erlotinib) at a flow rate of 1 mL/min for 25 min. The autosampler temperature was set at 4°C. The calibration curves for erlotinib, OSI420, and gefitinib were constructed over the concentration ranges of 0.8 to 50, 0.2 to 13, and 1.5 to 50 μmol/L, respectively. The within- and between-day precision and accuracies were <15%.

High-performance liquid chromatography with tandem mass spectrometric detection was used to identify the chemical structure of one

major metabolite (M5) of erlotinib from the CYP1A1 reaction mixture. The separation was done on a 3.9 × 150 mm SymmetryShield $RP_8$ column (Waters) with a mobile phase consisting of 1% formic acid in acetonitrile-10 μmol/L ammonium acetate (32/68, v/v). The eluent was monitored using mass spectrometry scan mode (200-400 amu), under the following mass spectrometric conditions: source temperature of 120°C, desolvation temperature of 350°C, cone voltage of 40 V, and capillary voltage of 300 V.

***Effects of gefitinib and erlotinib on midazolam metabolism in human liver and intestinal microsomes.*** Midazolam, a probe substrate for human CYP3A, was incubated in pooled human liver or intestinal microsomes in the presence or absence of gefitinib or erlotinib. A 0.2-mL reaction mixture contained midazolam 20 μmol/L with or without gefitinib or erlotinib (0, 1, 5, and 20 μmol/L), 1.3 mmol/L $NADP^+$, 3.3 mmol/L glucose-6-phosphate, 0.4 units/mL glucose-6-phosphate dehydrogenase, 3.3 mmol/L magnesium chloride, and pooled human liver or intestinal microsomes (protein concentration, 0.5 mg/mL), in 100 mmol/L potassium phosphate buffer (pH 7.4). Reaction mixtures were incubated at 37°C for 20 min and terminated by adding 0.1 mL acetonitrile and centrifuging at 14,000 rpm at 4°C for 10 min. The supernatant was collected and stored at -80°C until analysis. The control incubation with inactivated microsomes was done simultaneously. The coincubation of midazolam with imatinib, a reported CYP3A4 inhibitor (10), in human liver microsomes was used as an experimental control.

Midazolam and 1-hydroxymidazolam were measured using a validated method based on high-performance liquid chromatography with tandem mass spectrometric detection, as described previously (7).

***Data analysis.*** Substrate disappearance velocity ($v$) was calculated as [($C_{s,initial}$ - $C_{s,30\ min}$) / incubation time / CYP concentration], where $C_{s,initial}$ was substrate concentration at time 0 and $C_{s,30\ min}$ was the substrate concentration after a 30-min incubation with the various CYP Supersomes. Metabolite formation velocity ($v$) was calculated as ($C_{m,30\ min}$ / incubation time / CYP concentration), where $C_{m,30\ min}$ was the metabolite concentration after a 30-min incubation. Plots of substrate concentration ($X$ axis) versus $v$ ($Y$ axis) were then constructed. The kinetic profiles of the substrate disappearance and metabolite formation were fitted by a Michaelis-Menten equation (Eq. A), linear sum of two Michealis-Menten functions (Eq. B), or Hill equation (Eq. C). The choice of enzyme kinetic models was guided by visual inspection of the substrate concentration-velocity plots and corresponding Eadie-Hofstee plots. The model discrimination between a complex model and a simpler one was based on statistical "goodness-of-fit" including the Akaike Information Criteria and $F$ test (11). All fittings were done using WinNonlin 5.0 (Pharsight Corporation).

$$v = \frac{V_{max} \times S}{K_m + S} \quad (A)$$

$$v = \frac{V_{max} \times S}{K_m + S} + Cl_{int2} \times S \quad (B)$$

$$v = \frac{V_{max} \times S^n}{S_{50}^{\ n} + S^n} \quad (C)$$

$$Cl_{max} = \frac{V_{max}}{S_{50}} \times \frac{(n-1)}{n \times (n-1)^{1/n}} \quad (D)$$

$$Cl_{int} = \frac{V_{max}}{K_m} + Cl_{int2} \quad (E)$$

In these equations, $S$ is substrate concentration, $V_{max}$ is maximum metabolite formation or substrate disappearance velocity, $K_m$ or $S_{50}$ is the substrate concentration at which 50% of $V_{max}$ is obtained, $Cl_{int2}$ is an estimate of the low-affinity intrinsic clearance, and $n$ is the Hill coefficient. The maximum clearance ($Cl_{max}$), calculated from Eq. D, provides an estimate of the highest clearance attained as substrate concentration increases before any saturation of the enzyme sites. The intrinsic clearance ($Cl_{int}$) was equal to the $V_{max}/K_m$ ratio for the process consistent with a Michaelis-Menten kinetics, and equal to the sum of the high- and low-affinity clearance terms (Eq. E) for the process described by the two Michaelis-Menten kinetics.

**Table 1.** Enzyme kinetic variables for CYP3A4-, CYP3A5-, CYP2D6-, CYP1A1-, and CYP1A2-mediated metabolism of gefitinib and erlotinib

| | CYP3A4 | CYP3A5 | CYP2D6 | CYP1A1 | CYP1A2 |
|---|---|---|---|---|---|
| Disappearance of gefitinib* | | | | | |
| $V_{max}$ (nmol/min/nmol CYP) | 20.8 (5.9%) | 28.0 (11.1%) | 21.7 (13.1%) | 19.2 (4.9%) | ND |
| $S_{50}$ (μmol/L) | 25.7 (8.5%) | 43.7 (20.3%) | 24.7 (28.5%) | 24.5 (23.5%) | ND |
| $n$ | 2.05 (12.8%) | 1.26 (9.9%) | 9.91 (35.4%) | 10.0 (30.1%) | ND |
| $Cl_{max}$ (mL/min/nmol CYP) † | 0.41 | 0.39 | 0.63 | 0.57 | ND |
| Disappearance of erlotinib* | | | | | |
| $V_{max}$ (nmol/min/nmol CYP) | 4.17 (5.2%) | 4.49 (4.1%) | 4.08 (15.6%) | 3.99 (8.1%) | 4.61 (5.5%) |
| $S_{50}$ (μmol/L) | 9.0 (9.7%) | 11.8 (8.4%) | 26.9 (25.5%) | 7.09 (17.8%) | 15.4 (8.4%) |
| $n$ | 1.68 (11.9%) | 1.40 (7.4%) | 1.44 (14.2%) | 3.38 (54.5%) | 1.93 (10.7%) |
| $Cl_{max}$ (mL/min/nmol CYP) † | 0.24 | 0.21 | 0.08 | 0.31 | 0.15 |
| Formation of OSI-420 ‡ | | | | | |
| $V_{max}$ (nmol/min/nmol P450) | 0.14 (22.6%) | 0.36 (46.0%) | 0.43 (6.2%) | 0.29 (17.9%) | 0.27 (14.4%) |
| $K_m$ (μmol/L) | 1.74 (71.8%) | 9.50 (66.5%) | 10.2 (17.1%) | 13.5 (56.8%) | 8.96 (44.3%) |
| $Cl_{int2}$ (mL/min/nmol P450) | 0.01 | 0.01 | | — | — |
| $Cl_{int}$ (mL/min/nmol P450)§ | 0.09 | 0.05 | 0.04 | 0.02 | 0.03 |

NOTE: Data are the variable estimates and the coefficient of variation of the estimate is provided in parentheses. ND indicates that gefitinib was metabolized by CYP1A2 to a negligible extent.
Abbreviation: ND, not determined.
*Kinetic variables were obtained from the fittings of pooled data from two or three experiments to the Hill equation.
† Calculated from Eq. D.
‡ Kinetic variables were obtained from the fittings of pooled data from two or three experiments to the one or two Michaelis-Menten function.
§Calculated from Eq. E.

## Results

Gefitinib was metabolized by CYP3A4, CYP3A5, CYP2D6, and CYP1A1, and to a negligible extent by CYP1A2 and CYP1B1 (Fig. 1A); the formation of *O*-desmethyl-gefitinib, the major metabolite observed in human plasma (6), was mediated by CYP2D6 (Fig. 1C). The overall metabolism of erlotinib and formation of *O*-desmethyl-erlotinib (OSI-420), the major metabolite observed in human plasma (4), was mediated primarily by CYP3A4, CYP3A5, and CYP1A1, to a lesser extent by CYP1A2 and CYP2D6, and to a negligible extent by CYP1B1 (Fig. 1B and D).

Enzyme kinetic variables for the overall metabolism of gefitinib and erlotinib were estimated by fitting the pooled data from two or three incubations with CYP3A4, CYP3A5, CYP2D6, CYP1A1, or CYP1A2 with the Hill equation. Table 1 presents the enzyme kinetic variables. The estimated *in vitro* maximum clearance ($Cl_{max}$) for overall gefitinib metabolism was 0.41, 0.39, 0.63, and 0.57 mL/min/nmol CYP by CYP3A4, CYP3A5, CYP2D6, and CYP1A1, respectively; the $Cl_{max}$ values for overall erlotinib metabolism were 0.24, 0.21, 0.08, 0.31, and 0.15 mL/min/nmol CYP by CYP3A4, CYP3A5, CYP2D6, CYP1A1, and CYP1A2 (Table 1). Enzyme kinetics for OSI-420 formation was fitted by one (for CYP 2D6, CYP1A1, and CYP1A2) or two (for CYP3A4 and CYP3A5) Michealis-Menten function(s). The estimated *in vitro* intrinsic clearance ($Cl_{int}$) for OSI-420 formation was 0.09, 0.05, 0.04, 0.02, and 0.03 mL/min/nmol CYP by CYP3A4, CYP3A5, CYP2D6, CYP1A1, and CYP1A2, respectively. Enzyme kinetics of *O*-desmethyl gefitinib was not determined because the reference standard of *O*-desmethyl gefitinib was not available in this study.

Figure 2 shows the high-performance liquid chromatograms of erlotinib and its metabolites in the incubations with its major metabolizing enzymes CYP3A4, CYP3A5, CYP1A1, and CYP1A2. The CYP3A4 and CYP3A5 incubations produced a similar metabolite profile. A novel erlotinib metabolite (M5) was identified in the CYP1A1 incubation reaction, which was not previously identified in human plasma, urine, or feces (4). Mass spectrometric analysis suggested that M5 had a protonated molecular ion at *m/z* 336, and a daughter ion at *m/z* 278. The ion at 336 (M5) could be due to the loss of a methoxyethyl group from erlotinib (*m/z*, 394) by CYP1A1 metabolism, and the daughter ion at 278 was the result of the loss of a methoxyethyl group from M5. The proposed chemical structure of M5 is presented in Fig. 2C.

Both gefitinib and erlotinib stimulated, in a concentration-dependent manner, the disappearance of midazolam and formation of 1-hydroxymidazolam, and erlotinib seemed to do this to a lesser extent in human liver and intestinal microsomes (Fig. 3). As shown in Table 2, in the presence of 20 μmol/L gefitinib or erlotinib, midazolam disappearance rate in liver microsomes at its initial concentration of 20 μmol/L was increased to 145% and 133% of control, respectively, and in intestinal microsome to 352% and 201% of control, respectively; correspondingly, 1-hydroxymidazolam formation rate was increased in liver microsomes to 207% and 125% of control, respectively, and in intestinal microsome to 215% and 118% of control, respectively. The control experiments with imatinib (a known CYP3A4 inhibitor) showed that imatinib reduced midazolam disappearance and 1-hydroxymidazolam formation by ~30% and 40% in liver microsomes, respectively (Table 2).

## Discussion

The *in vitro* metabolism studies described here provide the first data that quantitatively describes the kinetics of metabolism of gefitinib and erlotinib by individual CYP enzymes. *In vitro* maximum clearance by CYP3A4, CYP3A5, and CYP1A1 was ~2-fold higher for gefitinib than erlotinib, and the maximum clearance by CYP2D6 was ~8-fold higher for gefitinib. These *in vitro* findings indicate that erlotinib is less susceptible than gefitinib to metabolism by major liver CYP enzymes and this notion may explain the pharmacokinetic data in cancer patients showing lower apparent oral clearance for erlotinib compared with gefitinib (4.0 versus 21 L/h; refs. 7, 8). As a result, higher plasma erlotinib exposure is achieved, despite administration of a lower erlotinib daily dose compared with gefitinib (150 versus 250 mg). The approved gefitinib dose is approximately one third of the MTD, whereas erlotinib is

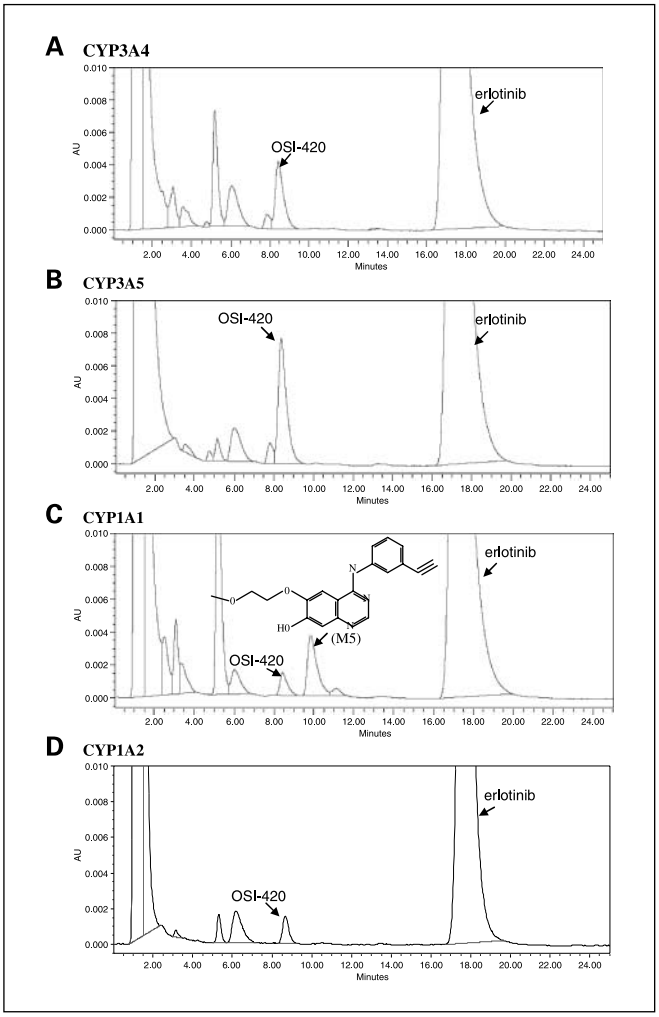


**Fig. 2.** High-performance liquid chromatograms of the incubation mixture of erlotinib (50 μmol/L) with CYP3A4 (*A*), CYP3A5 (*B*), CYP1A1 (*C*), and CYP1A2 (*D*) at a CYP concentration of 100 pmol/mL at 37°C for 30 min. Erlotinib and metabolites were monitored at a wavelength of 246 nm.

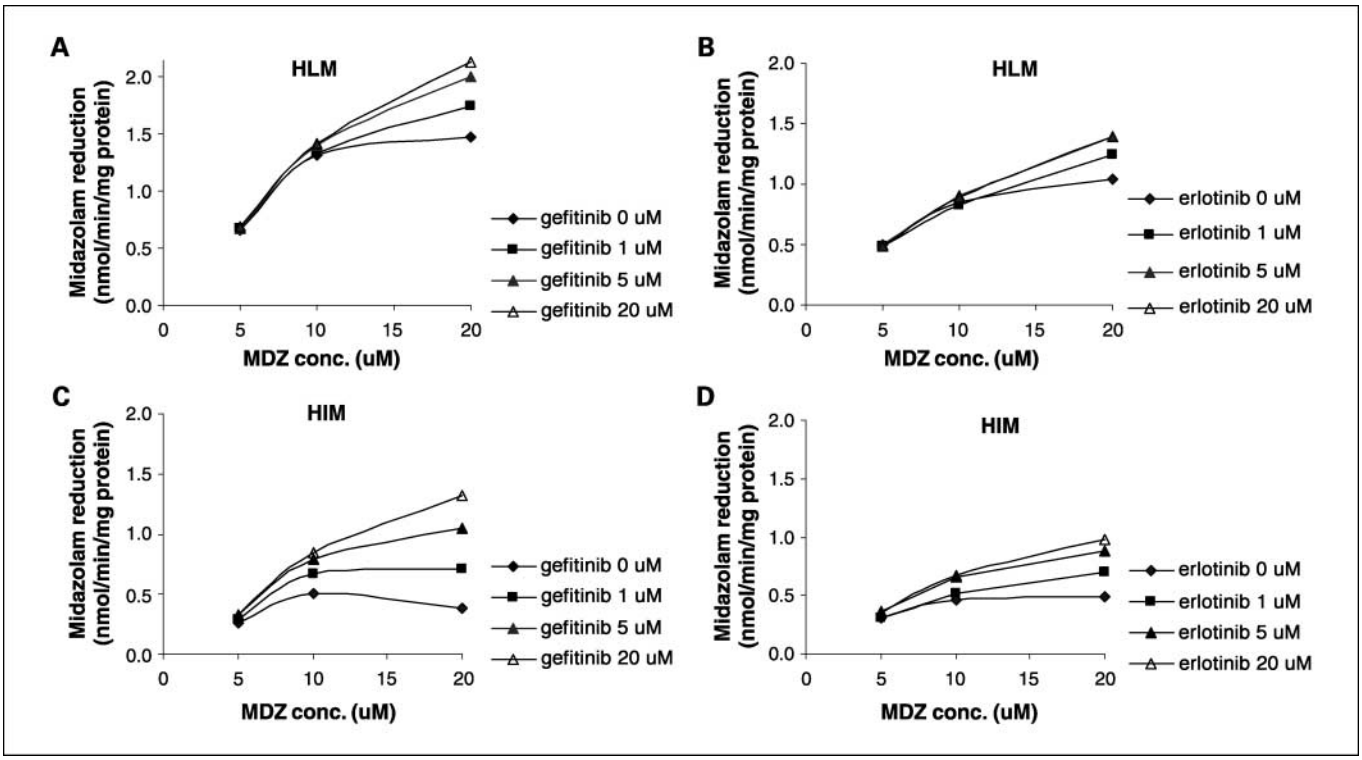


**Fig. 3.** Velocity versus substrate concentration plots of midazolam (*MDZ*) disappearance (reduction) in the absence and presence of gefitinib (*A* and *C*) or erlotinib (*B* and *D*) in human liver microsomes (*HLM*; *A* and *B*) and human intestinal microsomes (*HIM*; *C* and *D*). Points, mean of duplicate determinations (with coefficient variation <15%).

administered at its MTD (12). The use of erlotinib at its MTD along with a lower apparent oral clearance results in 3.5-fold higher systemic exposure than gefitinib and may provide a clinical advantage for erlotinib over gefitinib.

In addition to CYP3A4 and CYP3A5, CYP1A isozymes may represent another important pathway in the hepatic and extrahepatic metabolism of both gefitinib and erlotinib. As shown in Table 1, CYP1A1 exhibited a higher *in vitro* maximum clearance than CYP3A4 and CYP3A5 for both drugs. CYP1A1 is expressed predominantly in extrahepatic organs, and is inducible by aryl hydrocarbon receptor ligands and cigarette smoking in extrahepatic tissues as well as in the liver (13, 14). In addition, CYP1A2 was involved in the metabolism of erlotinib, but not gefitinib (Fig. 1; Table 1). CYP1A2 is specifically expressed in the liver, constituting ~13% of the total hepatic CYP content (15). Like CYP1A1, CYP1A2 is inducible by cigarette smoking and other factors (16). Recently, smoking status was found to be associated with higher erlotinib clearance (17). The lower erlotinib systemic exposure observed in smokers may have been due, in part, to induction of CYP1A2 and possibly CYP1A1 in the liver. The effect of smoking status on the pharmacokinetics of gefitinib has not been evaluated. Never-smoking status has been identified as an important clinical predictor for favorable response to both gefitinib and erlotinib (18). Although somatic

**Table 2.** Effects of gefitinib and erlotinib on the disappearance of midazolam and formation of 1-hydroxymidazolam in human liver and intestinal microsomes

| | Midazolam disappearance rate (% of control) | | | 1-Hydroxymidazolam formation rate (% of control) | | |
|---|---|---|---|---|---|---|
| | Gefitinib | Erlotinib | Imatinib | Gefitinib | Erlotinib | Imatinib |
| Liver microsomes (μmol/L) | | | | | | |
| 1 | 119 | 119 | 87 | 128 | 99 | 71 |
| 5 | 136 | 134 | 79 | 185 | 129 | 74 |
| 20 | 145 | 133 | 70 | 207 | 125 | 59 |
| Intestinal microsomes (μmol/L) | | | | | | |
| 1 | 188 | 145 | ND | 131 | 88 | ND |
| 5 | 280 | 181 | ND | 197 | 135 | ND |
| 20 | 352 | 201 | ND | 215 | 118 | ND |

NOTE: Values are presented as the mean of duplicate determinations. Midazolam initial concentration was 20 μmol/L. The control was midazolam disappearance rate or 1-hydroxymidazolam formation rate in the absence of an effector (e.g., gefitinib, erlotinib, or imatinib). Imatinib (a reported CYP3A inhibitor) was used as the control experiment.

*EGFR* mutations have been observed more frequently in never smokers compared with ever smokers (19, 20) and likely provides an explanation for better response to EGFR tyrosine kinase inhibitors in this patient population, a better treatment outcome could also be attributed, in part, to higher tumoral drug exposure in nonsmokers. CYP1A1, presenting in tumors, may play a key role in the tumoral metabolism of gefitinib and erlotinib, and, therefore, smoking induction of CYP1A1 could lead to increased tumoral metabolism and decreased exposure to the pharmacologically active parent drug. It is worth noting that a major erlotinib metabolite (named M5 here) in the CYP1A1 incubation was identified by mass spectrometry (Fig. 3C). M5 was not identified in human plasma, feces, or urine, suggesting that it could be a specific tumoral metabolite of erlotinib formed by CYP1A1. The EGFR tyrosine kinase inhibitory activity of M5 is yet to be determined, but it is likely less potent than erlotinib.

The comparative enzyme kinetic data suggest that gefitinib and erlotinib may have different drug-drug interaction potentials. Both drugs were metabolized mainly by CYP3A4 and CYP3A5, and, therefore, CYP3A4/A5 inhibitors or inducers may significantly alter their oral clearance and systemic or tumoral exposures. For example, it has been found that a single-dose administration of rifampicin (a potent CYP3A4 inducer) and itraconazole (a potent CYP3A4 inhibitor) significantly reduced and increased gefitinib systemic exposure by 83% and 78%, respectively (21). Likewise, CYP3A4/3A5 inducers and inhibitors may alter erlotinib systemic exposure as well. However, if administered chronically in combination with an inhibitor of CYP3A4/5, erlotinib may be more susceptible than gefitinib to altered metabolism and clearance because an alternative pathway such as CYP2D6 could play a more prominent role in overall gefitinib clearance in the presence of continued CYP3A4 inhibition. For instance, this could be important if a platelet-derived growth factor receptor inhibitor, such as imatinib, which is also a CYP3A4 inhibitor, is combined with an EGFR tyrosine kinase inhibitor, a combination that has potential utility for the treatment of a variety of cancers and lung diseases (22).

Gefitinib and erlotinib may act as stimulators that influence the metabolism of other CYP3A4/A5 substrates. As shown in the *in vitro* studies, both drugs stimulated the disappearance of midazolam and formation of 1′-hydroxymidazolam in human liver and intestinal microsomes (Table 2). Although gefitinib appeared to stimulate midazolam metabolism to a greater extent than erlotinib, the few data points limit a rigorous statistical comparison between the two drugs. A previous report showed a stimulatory effect of gefitinib on midazolam hydroxylation in human liver microsomes and the effect seemed to be similar to that observed with α-naphthoflavone (23). Proposed mechanisms for activation of CYP3A-catalyzed oxidative metabolism includes the allosteric site model and two substrate binding site models (24, 25). The detailed mechanism by which gefitinib and erlotinib stimulated CYP3A4/A5–mediated metabolism of midazolam is unknown. One possible explanation could be that gefitinib or erlotinib bind to an allosteric site on the CYP3A protein, which causes a conformational change in the midazolam binding pocket, which then increased the coupling efficiency of midazolam to CYP3A4/3A5. Stimulation of CYP3A4-mediated oxidation reactions is likely substrate dependent, and it is unknown if gefitinib and erlotinib induce their own metabolism and thus affect their own oral bioavailability and systemic clearance.

In conclusion, gefitinib is more susceptible to CYP-mediated metabolism than erlotinib, which may contribute to increased gefitinib apparent oral clearance and lower systemic exposures achieved relative to erlotinib. CYP1A may represent an important pathway in the hepatic and extrahepatic metabolism of both drugs and a determinant of pharmacokinetic variability and drug response. The differential metabolizing enzyme profiles suggest that there may be differences in drug-drug interaction potential between erlotinib and gefitinib, and stimulation of CYP3A4 may likely play a role in drug interactions with both agents. The present findings shed light on mechanisms underlying variability in drug exposure and clinical effects for the EGFR tyrosine kinase inhibitors gefitinib and erlotinib.

## References


1. Siegel-Lakhai WS, Beijnen JH, Schellens JH. Current knowledge and future directions of the selective epidermal growth factor receptor inhibitors erlotinib (Tarceva) and gefitinib (Iressa). Oncologist 2005;10:579–89.
2. Frohna P, Lu J, Eppler S, et al. Evaluation of the absolute oral bioavailability and bioequivalence of erlotinib, an inhibitor of the epidermal growth factor receptor tyrosine kinase, in a randomized, crossover study in healthy subjects. J Clin Pharmacol 2006;46:282–90.
3. Swaisland HC, Smith RP, Laight A, et al. Single-dose clinical pharmacokinetic studies of gefitinib. Clin Pharmacokinet 2005;44:1165–77.
4. Ling J, Johnson KA, Miao Z, et al. Metabolism and excretion of erlotinib, a small molecule inhibitor of epidermal growth factor receptor tyrosine kinase, in healthy male volunteers. Drug Metab Dispos 2006;34:420–6.
5. McKillop D, McCormick AD, Millar A, Miles GS, Phillips PJ, Hutchison M. Cytochrome P450-dependent metabolism of gefitinib. Xenobiotica 2005;35:39–50.
6. McKillop D, Hutchison M, Partridge EA, et al. Metabolic disposition of gefitinib, an epidermal growth factor receptor tyrosine kinase inhibitor, in rat, dog and man. Xenobiotica 2004;34:917–34.
7. Li J, Karlsson MO, Brahmer J, et al. CYP3A phenotyping approach to predict systemic exposure to EGFR tyrosine kinase inhibitors. J Natl Cancer Inst 2006;98:1714–23.
8. Lu JF, Eppler SM, Wolf J, et al. Clinical pharmacokinetics of erlotinib in patients with solid tumors and exposure-safety relationship in patients with non-small cell lung cancer. Clin Pharmacol Ther 2006;80:136–45.
9. Tan AR, Yang X, Hewitt SM, et al. Evaluation of biologic end points and pharmacokinetics in patients with metastatic breast cancer after treatment with erlotinib, an epidermal growth factor receptor tyrosine kinase inhibitor. J Clin Oncol 2004;22:3080–90.
10. Peng B, Lloyd P, Schran H. Clinical pharmacokinetics of imatinib. Clin Pharmacokinet 2005;44:879–94.
11. Venkatakrishnan K, Schmider J, Harmatz JS, et al. Relative contribution of CYP3A to amitriptyline clearance in humans: *in vitro* and *in vivo* studies. J Clin Pharmacol 2001;41:1043–54.
12. Blackhall F, Ranson M, Thatcher N. Where next for gefitinib in patients with lung cancer? Lancet Oncol 2006;7:499–507.
13. Bowen WP, Carey JE, Miah A, et al. Measurement of cytochrome P450 gene induction in human hepatocytes using quantitative real-time reverse transcriptase-polymerase chain reaction. Drug Metab Dispos 2000;28:781–8.
14. Iba MM, Fung J. Induction of pulmonary cytochrome P4501A1: interactive effects of nicotine and mecamylamine. Eur J Pharmacol 1999;383:399–403.
15. Imaoka S, Yamada T, Hiroi T, et al. Multiple forms of human P450 expressed in *Saccharomyces cerevisiae*. Systematic characterization and comparison with those of the rat. Biochem Pharmacol 1996;51:1041–50.
16. Landi MT, Sinha R, Lang NP, Kadlubar FF. Human cytochrome P4501A2. IARC Sci Publ 1999;173–95.
17. Hamilton M, Wolf JL, Rusk J, et al. Effects of smoking on the pharmacokinetics of erlotinib. Clin Cancer Res 2006;12:2166–71.
18. Janne PA, Johnson BE. Effect of epidermal growth factor receptor tyrosine kinase domain mutations on the outcome of patients with non-small cell lung cancer treated with epidermal growth factor receptor tyrosine kinase inhibitors. Clin Cancer Res 2006;12:4416–20s.

**19.** Pao W, Miller V, Zakowski M, et al. EGF receptor gene mutations are common in lung cancers from "never smokers" and are associated with sensitivity of tumors to gefitinib and erlotinib. Proc Natl Acad Sci U S A 2004;101:13306–11.
**20.** Shigematsu H, Lin L, Takahashi T, et al. Clinical and biological features associated with epidermal growth factor receptor gene mutations in lung cancers. J Natl Cancer Inst 2005;97:339–46.
**21.** Swaisland HC, Ranson M, Smith RP, et al. Pharmacokinetic drug interactions of gefitinib with rifampicin, itraconazole and metoprolol. Clin Pharmacokinet 2005;44:1067–81.
**22.** Ingram JL, Bonner JC. EGF and PDGF receptor tyrosine kinases as therapeutic targets for chronic lung diseases. Curr Mol Med 2006;6:409–21.
**23.** Fujita K, Ando Y, Narabayashi M, et al. Gefitinib (Iressa) inhibits the CYP3A4-mediated formation of 7-ethyl-10-(4-amino-1-piperidino)carbonyloxycamptothecin but activates that of 7-ethyl-10-[4-*N*-(5-aminopentanoic acid)-1-piperidino]carbonyloxycamptothecin from irinotecan. Drug Metab Dispos 2005;33:1785–90.
**24.** Shou M, Grogan J, Mancewicz JA, et al. Activation of CYP3A4: evidence for the simultaneous binding of two substrates in a cytochrome P450 active site. Biochemistry 1994;33:6450–5.
**25.** Ueng YF, Kuwabara T, Chun YJ, Guengerich FP. Cooperativity in oxidations catalyzed by cytochrome P450 3A4. Biochemistry 1997;36:370–81.

Clinical Cancer Research

# Differential Metabolism of Gefitinib and Erlotinib by Human Cytochrome P450 Enzymes

Jing Li, Ming Zhao, Ping He, et al.

*Clin Cancer Res* 2007;13:3731-3737.